# Organoplatinum Polymorphs with Varying Molecular Conformation, Intermolecular Interaction, and Luminescence

Dong-Ren Bai and Suning Wang*

*Department of Chemistry, Queen's University, Kingston, Ontario, K7L 3N6, Canada*

*Received January 6, 2006*

Two mononuclear organoplatinum complexes based on the 2,2′-dipyridylamino derivative ligands (2,2′-dipyridylamino)phenyl triphenyl methane (dm) and (2,2′-dipyridylamino)phenyl triphenyl silane (dsi) with the formula $PtPh_2$(dm) (**1**) and $PtPh_2$(dsi) (**2**), respectively, have been synthesized. Both **1** and **2** have been found to form two polymorphs concomitantly: a colorless blue-luminescent form **A** (space group $I4_1/a$) (**1A** and **2A**) and a yellow nonluminescent form **B** (space group $P2_1/c$) (**1B** and **2B**). The crystal structures of **1A**, **1B**, and **2A** were determined by single-crystal X-ray diffraction analyses. The $CPh_3$ group was found to display different conformations in the crystal lattices of **1A** and **1B**. Considerable variations in intermolecular interactions were also observed for the crystals of **1A** and **1B**. **2A** was found to be isostructural to **1A**. Spectroscopic study (UV−vis and luminescence) and molecular orbital calculations (Gaussian98) were performed to understand the color and luminescent differences between **1A** and **1B**. Intermolecular $\pi-\pi$ stacking interactions between a phenyl of the $CPh_3$ group and the pyridyl of the 2,2′-dipyridylamino group were found to be the most likely cause for the absence of emission in the crystals of **1B**.

## Introduction

Luminescent organoplatinum complexes are an important class of molecules that have attracted much research interest because of their potential applications in chemical sensors[1] and photocatalysts.[2,3] The demonstration by Thompson and co-workers that luminescent platinum complexes can be used as highly efficient phosphorescent emitters in organic light emitting devices (OLEDs) has further stimulated the research interests and activities in phosphorescent organoplatinum compounds.[4] Because the operating mechanism of OLEDs involves charge injection, charge recombination, and exciton relaxation via the emission of photons, intermolecular interactions and the morphology of the molecular layers in the device play a vital role in the performance of the device.[5] Therefore, understanding the relationship between molecular structures, molecular interactions, and electronic/photophysical properties is very important for the advancement of OLEDs and other relevant fields. Although polymorphs that display distinct electronic properties are known in organic compounds,[6] well-established examples involving organometallic compounds, especially organoplatinum compounds, remain scarce. Most previously reported polymorphs of platinum complexes or organoplatinum compounds that display distinct electronic properties are caused by weak metal···metal interactions,[7] which have found potential uses as sensors for organic solvents/vapors due to the sensitivity of the degree of weak metal−metal association/interaction to certain organic molecules.[7] A few examples of polymorphs by platinum complexes that differ in either the conformation or intermolecular interactions of the ligands are known; however no distinct

(1) (a) Peyratout, C. S.; Aldridge, T. K.; Crites, D. K.; McMillin, D. R. *Inorg. Chem.* **1995**, *34*, 4484. (b) Houlding, V. H.; Frank, A. J. *Inorg. Chem.* **1985**, *24*, 3664. (c) Kunugi, Y.; Mann, K. R.; Miller, L. L.; Exstrom, C. L. *J. Am. Chem. Soc.* **1998**, *120*, 589. (d) Yam, V. W.-W.; Tang, R. P.-L.; Wong, K. M.-C.; Ko, C.-C.; Cheung, K.-K. *Inorg. Chem.* **2001**, *40*, 571. (e) Wong, K. M.-C.; Tang, W.-S.; Lu, X.-X.; Zhu, N.; Yam, V. W.-W. *Inorg. Chem.* **2005**, *44*, 1492.

(2) (a) Zhang, D.; Wu, L.-Z.; Zhou, L.; Han, X.; Yang, Q.-Z.; Zhang, L.-P.; Tung, C.-H. *J. Am. Chem. Soc.* **2004**, *126*, 3440. (b) Connick, W. B.; Gray, H. B. *J. Am. Chem. Soc.* **1997**, *119*, 11620. (c) Hissler, M.; McGarrah, J. E.; Connick, W. B.; Geiger, D. K.; Cummings, S. D.; Eisenberg, R. *Coord. Chem. Rev.* **2000**, *208*, 115.

(3) (a) Islam, A.; Sugihara, H.; Hara, K.; Singh, L. P.; Katoh, R.; Yanagida, M.; Takahashi, Y.; Murata, S.; Arakawa, H.; Fujihashi, G. *Inorg. Chem.* **2001**, *40*, 5371. (b) McGarrah, J. E.; Kim, Y. J.; Hissler, M.; Eisenberg, R. *Inorg. Chem.* **2001**, *40*, 4510. (c) McGarrah, J. E.; Eisenberg, R. *Inorg. Chem.* **2003**, *42*, 4355.

(4) (a) Baldo, M. A.; O'Brien, D. F.; You, Y.; Shoustikov, A.; Sibley, S.; Thompson, M. E.; Forrest, S. R. *Nature* **1998**, *395*, 151. (b) Kwong, R. C.; Sibley, S.; Dubovoy, T.; Baldo, M.; Forrest, S. R.; Thompson, M. E. *Chem. Mater.* **1999**, *11*, 3709. (c) Kwong, R. C.; Lamansky, S.; Thompson, M. E. *Adv. Mater.* **2000**, *12*, 1134. (d) Lu, W.; Mi, B. X.; Chan, M. C. W.; Hui, Z.; Zhu, N.; Lee, S. T.; Che, C. M. *Chem. Commun.* **2002**, 206. (e) Liu, Q.; Thorne, L.; Kozin, I.; Song, D.; Seward, C.; D'Iorio, M.; Tao, Y.; Wang, S. *J. Chem. Soc., Dalton Trans.* **2002**, 3234. (f) Liu, Q.; Jia, W. L.; Wu, G.; Wang, S. *Organometallics* **2003**, *23*, 3781. (g) Lu, W.; Mi, B.-X.; Chan, M. C. W.; Hui, Z.; Che, C.-M.; Zhu, N.; Lee, S.-T. *J. Am. Chem. Soc.* **2004**, *126*, 4958. (h) Liu, Q.; Jia, W. L.; Wang, S. *Inorg. Chem.* **2005**. *44*, 1332.

(5) (a) Kim, T. S.; Okubo, T.; Mitani, T. *Chem. Mater.* **2003**, *15*, 4949. (b) Muccini, M.; Loi, M. A.; Kenevey, K.; Zamboni, R.; Masciocchi, N.; Sironi, A. *Adv. Mater.* **2004**, *16*, 861. (c) Tsutsui, T. *Mater. Res. Soc. Bull.* **1997**, *22* (6), 39. (d) Chen, C. J.; Shi, J. *Coord. Chem. Rev.* **1998**, *171*, 161. (e) Hu, N. X.; Esteghamatian, M.; Xie, S.; Popovic, Z.; Hor, A. M.; Ong, B.; Wang, S. *Adv. Mater.* **1999**, *11*, 17. (f) Yase, K.; Yoshida, Y.; Sumimoto, S.; Tanigaki, N.; Matsuda, H.; Kato, M. *Thin Solid films* **1996**, *273*, 218. (g) Smith, P. F.; Gerroir, P.; Xie, S.; Hor, A. M.; Popovic, Z.; Hair, M. L. *Langmuir* **1998**, *14*, 5946. (h) Sato, Y. in *Electroluminescence I*; Meuller, G., Ed.; Academic Press: San Diego, 1999; Vol. 64, Chapter 4, p 209.

(6) (a) Bernstein, J. *J. Phys. D: Appl. Phys.* **1993**, *26*, B66. (b) Bernstein, J.; Davey, R. J.; Henck, J. *Angew. Chem., Int. Ed.* **1999**, *38*, 3440. (c) Braga, D.; Grepioni, F. *Chem. Soc. Rev.* **2000**, *29*, 229. (d) Dunitz, J. D.; Bernstein, J. *Acc. Chem. Res.* **1995**, *28*, 193.

(7) (a) Morgan, G. T.; Burstall, F. H. *J. Chem. Soc.* **1934**, 965. (b) Osborn, R. S.; Rogers, D. *J. Chem. Soc., Dalton Trans.* **1974**, 1002. (c) Herber, R. H.; Croft, M.; Coyer, M. J.; Bilash, B.; Sahiner, A. *Inorg. Chem.* **1994**, *33*, 2422. (d) Achar, S.; Catalano, V. J. *Polyhedron* **1997**, *16*, 1555. (e) Stork, J. R.; Olmstead, M. M.; Balch, A. L. *J. Am. Chem. Soc.* **2005**, *127*, 6512. (f) Yam, V. W.-W.; Wong, K. M.-C.; Zhu, N. *J. Am. Chem. Soc.* **2002**, *124*, 6506. (g) Connick, W. B.; Marsh, R. E.; Schaefer, W. P.; Gray, H. B. *Inorg. Chem.* **1997**, *36*, 913. (h) Wadas, T. J.; Wang, Q. M.; Kim, Y. J.; Flaschenreim, C.; Blanton, T. N.; Eisenberg, R. *J. Am. Chem. Soc.* **2004**, *126*, 16841. (i) Charmant, J. P. H.; Forniés, J.; Gómez, J.; Lalinde, E.; Merino, R. I.; Moreno, M. T.; Orpen, A. G. *Inorg. Chem.* **1979**, *18*, 3353.

10.1021/om0600184 CCC: $33.50 
Publication on Web 02/10/2006

color or electronic properties were observed.[8] We report herein two new organoplatinum complexes, $PtPh_2$(dm) (**1**) and $PtPh_2$-(dsi) (**2**) (dm = [*p*-(2,2′-dipyridylamino)phenyl]triphenylmethane,[9] dsi = [*p*-(2,2′-dipyridylamino)phenyl]triphenylsilane[9]), that display concomitant conformational polymorphs with distinct electronic properties and luminescence. To the best of our knowledge, this is the first report of concomitant conformational polymorphs of Pt(II) complexes that do not involve Pt···Pt interactions in the crystal lattice and display distinct luminescent properties.

## Experimental Section

**General Procedures.** All starting materials were purchased from Aldrich Chemical Co. and were used without further purification. Solvents were freshly distilled over appropriate drying reagents. $^1$H and $^{13}$C NMR spectra were recorded on Bruker Avance 400 spectrometers. Excitation and emission spectra were recorded on a Photon Technologies International QuantaMaster Model C60 spectrometer. Emission lifetime was measured on a Photon Technologies International Phosphorescent lifetime spectrometer, Timemaster C-631F equipped with a Xenon flash lamp, and digital emission photon multiplier tube using a band pathway of 5 nm for excitation and 2 nm for emission. The delay time used in the recording of the phosphorescent spectra is in the range 100 to 2000 $\mu$s. UV−vis spectra were recorded on a Hewlett-Packard 8562A diode array spectrophotometer. The samples for the solid-state UV−vis spectral measurements were prepared by grinding the crystals, then sandwiching them between two sapphire slides. Elemental analyses were performed by Canadian Microanalytical Service Ltd., Delta, British Columbia, Canada. Melting points were determined on a Fisher-Johns melting point apparatus. The Pt(II) starting material $[PtPh_2(SMe_2)]_n$ ($n$ = 2 or 3) and the free ligands dm and dsi were synthesized by previously reported procedures.[9,10]

**Synthesis of $PtPh_2$(dm) (1).** A solution of the dm ligand (0.013 g, 0.026 mmol) in 3 mL of $CH_2Cl_2$ was mixed with a solution of $PtPh_2(SMe_2)$ (0.013 g, 0.028 mmol) and stirred for 15 min. The mixture was filtered and layered with hexane and was allowed to stand for a few days. Colorless crystals (**1A**) and yellow crystals (**1B**) of $PtPh_2$(dm) (∼1:1 ratio) were obtained in 70% yield. The colorless crystals and the light yellow crystals were separated by hand-picking under a microscope. Mp: >300 °C (dec). $^1$H NMR in $CD_2Cl_2$ ($\delta$, ppm, 25° C): 8.47 (d, 2H), 7.92 (d, 2H), 7.66 (d, 2H), 7.28 (m, 21H), 7.14 (t, 2H), 6.88 (m, 6H), 6.76 (t, 2H). $^{13}$C NMR in $CD_2Cl_2$ ($\delta$, ppm, 25 °C): 151.42, 146.83, 144.22, 144.02, 142.15, 139.19, 138.13, 132.10, 130.95, 127.76, 127.60, 126.50, 125.90, 124.24, 123.63, 121.32, 117.90, 64.51. Anal. Calcd for $C_{47}H_{37}N_3Pt/0.5H_2O$: C, 66.59(67.30): H, 4.49(4.41); N, 4.96(5.01) (the number in parentheses is based on the formula without the water molecule). Found: C, 66.27; H, 4.32; N, 4.81. (The crystals of **1** and **2** were submitted for CHN analyses. Seven repeated analyses were performed by the Canadian Microanalytical Service lab using various conditions, but the results consistently showed that the carbon content is low by 1−2%. Incomplete combustion or trapping of water molecules by the samples was suggested as possible causes by the analytical lab.)

**Synthesis of $PtPh_2$(dsi) (2).** A solution of dsi ligand (0.013 g, 0.026 mmol) in 3 mL of $CH_2Cl_2$ was mixed with a solution of $PtPh_2(SMe_2)$ (0.013 g, 0.028 mmol) and stirred for 15 min. The mixture was filtered and layered with hexane and was allowed to stand for a few days. Colorless crystals and light yellow crystals (∼1:1 ratio) of **2** were isolated in 60% yield. The colorless crystals (**2A**) and the light yellow crystals (**2B**) were separated by hand under a microscope. Mp: >300 °C (dec). $^1$H NMR in $CD_2Cl_2$ ($\delta$, ppm, 25 °C): 8.49 (d, 2H), 7.98 (d, 2H), 7.72 (d, 2H), 7.61 (m, 10H), 7.45 (m, 9H), 7.32 (d, 2H), 7.19 (t, 2H), 6.93 (d, 2H), 6.87-(t, 4H), 6.78 (t, 2H). $^{13}$C NMR in $CD_2Cl_2$ ($\delta$, ppm, 25 °C): 151.58, 139.30, 138.32, 138.13, 137.74, 136.30, 134.28, 129.63, 128.75, 128.10, 127.93, 127.03, 126.51, 124.89, 124.15, 121.39, 116.46. Anal. Calcd for $C_{46}H_{37}N_3PtSi/0.5H_2O$: C, 63.96 (64.62); H, 4.40 (4.33); N, 4.87 (4.91) (the number in parentheses is based on the formula without the water molecule; see notes above). Found: C, 62.42; H, 4.32; N, 4.81.

**X-ray Crystallographic Analysis.** All crystals were mounted on glass fibers for data collection. Data were collected on a Siemens P4 single-crystal X-ray diffractometer with a CCD-1000 detector and graphite-monochromated Mo K$\alpha$ radiation, operating at 50 kV and 30 mA. All data collection was carried out at ambient temperature. The 2$\theta$ data collection ranges are 3.00−57.00° for all compounds. No significant decay was observed in any samples. Data were processed on a PC using the Bruker SHELXTL software package (version 5.10) and are corrected for absorption effects. All structures were solved by direct methods. All non-hydrogen atoms were refined anisotropically. The positions of hydrogen atoms were either located directly from difference Fourier maps or calculated and their contributions in structural factor calculations were included. The crystal data are provided in Table 1.

**Table 1. Crystal Data for 1A, 1B, and 2A**

| | 1A | 1B | 2A |
|---|---|---|---|
| formula | $C_{47}H_{37}N_3Pt$ | $C_{47}H_{37}N_3Pt$ | $C_{46}H_{37}N_3PtSi$ |
| fw | 838.89 | 838.89 | 854.97 |
| $T$ (K) | 293 | 293 | 293 |
| space group | $I4_1/a$ | $P2_1/c$ | $I4_1/a$ |
| $a$ [Å] | a = 31.788(3) | a = 13.0073(14) | 31.83(2) |
| $b$ [Å] | a = 31.788(3) | b = 17.0269(18) | 31.83(2) |
| $c$ [Å] | c = 14.1341(18) | c = 17.1491(17) | 14.636(15) |
| α [deg] | 90 | 90 | 90 |
| $\beta$ [deg] | 90 | 106.916(2) | 90 |
| $\gamma$ [deg] | 90 | 90 | 90 |
| $V$ [Å$^3$] | 14282(2) | 3633.7(7) | 14825(22) |
| $Z$ | 16 | 4 | 16 |
| $d_{calcd}$ [g/cm$^{-3}$] | 1.561 | 1.533 | 1.532 |
| $\mu$ [mm$^{-1}$] | 3.968 | 3.899 | 3.855 |
| $2\theta_{max}$ [deg] | 46.66 | 46.52 | 56.76 |
| no. of rflns measd | 35 480 | 17 868 | 52 214 |
| no. of rflns used ($R_{int}$) | 5177 (0.1188) | 5193 (0.0455) | 8943 (0.0475) |
| no. of params | 464 | 460 | 460 |
| final $R$ ($I > 2\sigma(I)$) | | | |
| $R_1$[a] | 0.0336 | 0.0259 | 0.0278 |
| $wR_2$[b] | 0.0373 | 0.0358 | 0.0442 |
| $R$ (all data) | | | |
| $R_1$[a] | 0.0900 | 0.0523 | 0.0738 |
| $wR_2$[b] | 0.0427 | 0.0385 | 0.0500 |
| goodness of fit on $F^2$ | 0.682 | 0.786 | 0.844 |

[a] $R_1 = \sum[|F_o| - |F_c|]/\sum|F_o|$. [b] $wR_2 = \{\sum[w(F_o^2 - F_c^2)]/\sum(wF_o^2)\}^{1/2}$. $w = 1/[\sigma^2(F_o^2) + (0.075P)^2]$, where $P = [\max.(F_o^2,0) + 2F_c^2]/3$.

**Scheme 1**

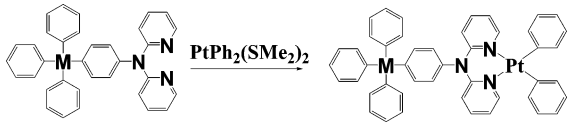


**1 M=C Pt(Ph)$_2$(dm)**
**2 M=Si Pt(Ph)$_2$(dsi)**

(8) (a) Jones, R.; Kelly, P. F.; Williams, D. J.; Woollins, J. D. *Dalton Trans.* **1988**, 1569. (b) Lippert, B.; Lock, C. J. L.; Speranzini, R. A. *Inorg. Chem.* **1981**, *20*, 335. (c) O'Connell, D.; Patterson, J. C.; Spalding, T. R.; Ferguson, G.; Gallagher, J. F.; Li, Y.; Kennedy, J. D.; Macias, R.; Thornton-Pett, M.; Holub, J. *Dalton Trans.* **1996**, 3323.

(9) Bai, D.-R. Wang, S. *Organometallics* **2004**, *23*, 5958.

(10) (a) Scott, J. D.; Puddephatt, R. J. *Organometallics* **1983**, *2*, 1643. (b) Hill, G. S.; Irwin, M. J.; Levy, C. J.; Rendina, L. M.; Puddephatt, R. J. *Inorg. Synth.* **1998**, *32*, 149. (c) Song, D.; Wang, S. *J. Organomet. Chem.* **2002**, *648*, 302.

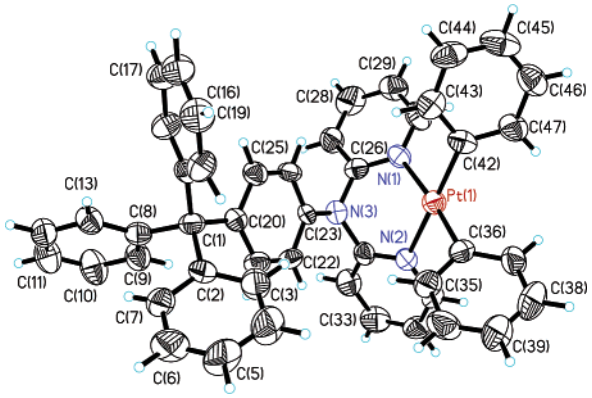


**Figure 1.** Diagram showing the molecular structure of **1A** with labeling schemes and thermal ellipsoids.

## Results and Discussion

**Syntheses and Characterization of 1 and 2.** The 2,2′-dipyridylamino-functionalized dm and dsi ligands were synthesized by using the procedure reported recently by our group.[9] The 2,2′-dipyridylamino group has been demonstrated by us and others to be very effective in chelating to metal ions such as Pt(II) and Zn(II).[4g,11] Indeed, the reaction of $[PtPh_2(SMe_2)]_n$ with the ligand dm or dsi in a 1:1 molar ratio yielded the corresponding Pt(II) complexes **1** and **2** readily and in good yield (Scheme 1), where the relatively labile bridging $SMe_2$ ligand in the Pt(II) starting material is replaced by the 2,2′-dipyridylamino moiety. An unusual observation is that two types of crystals, colorless ones (with a very light yellow tint) and yellow ones, coexist in the products of **1** and **2**. The colorless crystals (**1A** and **2A**) and the yellow crystals (**1B** and **2B**) were separated manually. $^1$H NMR data indicate that there is no difference between **1A** and **1B** (or **2A** and **2B**) in solution. Compounds **1** and **2** are stable in the solid state and in common solvents except $CHCl_3$ upon extended exposure to air. There appears a distinct solubility difference between the colorless crystals **1A** (**2A**) and the light yellow crystals **1B** (**2B**): the former has a poor solubility in $CH_2Cl_2$, $CH_3CN$, or DMSO, while the latter is fairly soluble in the same solvents. Attempts were made to determine the crystal structures of **1A**, **1B**, **2A**, and **2B** by single-crystal X-ray diffraction analyses. Single crystals suitable for X-ray analyses were obtained for **1A**, **1B**, and **2A**. In the case of **2B**, the crystals were too small to generate sufficient diffraction data.

**Crystal Structures of 1A, 1B, and 2A.** The molecular structure of **1A** with labeling schemes is shown in Figure 1 (the corresponding diagrams for **1B** and **2A** are provided in the Supporting Information). Important bond lengths and angles are given in Table 2. The space-filling diagrams for all three structures are shown in Figure 2. As shown by Figures 1 and 2, the coordination environments around the Pt(II) center in all three structures are similar: each Pt(II) center is bound by two nitrogen atoms of the 2,2′-dipyridylamino group and two phenyl groups in a *cis* fashion and a square planar geometry. The Pt−N and Pt−C bond lengths in all three structures do not vary significantly. However, there is a considerable variation of bond angles around the Pt(II) center for **1A** and **1B**. The Pt(II) center in **1A** appears to be more distorted from a square planar geometry than that of **1B**, as evidenced by the C(36)−Pt(1)−N(2) angle of 174.2(3)° (versus 177.0(2)° in **1B**). Furthermore, the methane carbon C(1) in **1A** and **1B** also displays considerable variations in bond angles. The pyridyl groups are nearly perpendicular to the central phenyl plane (Table 3). The amino nitrogen atom is conjugated with the central phenyl ring, as evidenced by the relatively short N−C(Ph) bond length (1.426(6) Å for **1A** and 1.419(5) Å for **1B**) and the small dihedral angle between the phenyl ring and the $NC_2$ plane (C is the carbon atom of the pyridyl ring attached to the amino nitrogen) (23.0° for **1A** and 34.1° for **1B**). The major difference between the molecular structures of **1A** and **1B** is the orientation of the three phenyl rings on the methane carbon. In **1A**, these three phenyl rings have an approximate propeller arrangement and their dihedral angles with the central phenyl ring range from 63.0° to 72.1° (see Table 3). In contrast, in **1B**, one of the phenyl rings is nearly perpendicular with the central phenyl ring (dihedral angle 88.2°), resulting in an approximate $C_s$ symmetry (the mirror plane goes through the Pt atom, the perpendicular phenyl, and the central phenyl ring) of the molecule. Consequently the molecular structures of **1A** and **1B** can be described as conformational polymorphs. The distance between the methane C(1) atom and the Pt atom is 6.96 and 6.51 Å for **1A** and **1B**, respectively.

In addition to the difference in molecular structure, **1A** and **1B** also display significant differences in molecular packing in the lattice, including Pt···H interactions and $\pi-\pi$ interactions. For **1A** there is a weak intermolecular interaction between the Pt(II) center and a hydrogen atom of a phenyl group (Pt···H = 2.93 Å) (Figure 3), resulting in a one-dimensional chain

**Table 2. Selected Bond Lengths (Å) and Angles (deg) for 1A, 1B, and 2A**

| compound **1A** | | compound **1B** | | compound **2A** | |
|---|---|---|---|---|---|
| Pt(1)−C(42) | 1.986(6) | Pt(1)−C(36) | 1.993(4) | Pt(1)−C(35) | 1.996(4) |
| Pt(1)−C(36) | 1.991(6) | Pt(1)−C(42) | 1.997(4) | Pt(1)−C(41) | 2.001(4) |
| Pt(1)−N(2) | 2.116(5) | Pt(1)−N(2) | 2.127(3) | Pt(1)−N(3) | 2.117(3) |
| Pt(1)−N(1) | 2.140(5) | Pt(1)−N(3) | 2.131(3) | Pt(1)−N(2) | 2.134(3) |
| C(1)−C(20) | 1.527(8) | C(1)−C(20) | 1.552(5) | Si−C(13) | 1.862(4) |
| C(1)−C(2) | 1.555(8) | C(1)−C(14) | 1.552(6) | Si−C(19) | 1.866(4) |
| C(1)−C(14) | 1.573(8) | C(1)−C(8) | 1.554(6) | Si−C(1) | 1.875(4) |
| C(1)−C(8) | 1.576(8) | C(1)−C(2) | 1.555(5) | Si−C(7) | 1.875(4) |
| C(42)−Pt(1)−C(36) | 93.9(3) | C(36)−Pt(1)−C(42) | 91.41(19) | C(35)−Pt(1)−C(41) | 92.80(14) |
| C(42)−Pt(1)−N(2) | 173.4(2) | C(36)−Pt(1)−N(2) | 175.87(16) | C(35)−Pt(1)−N(3) | 173.97(12) |
| C(36)−Pt(1)−N(2) | 91.9(2) | C(42)−Pt(1)−N(2) | 92.61(18) | C(41)−Pt(1)−N(3) | 92.82(12) |
| C(42)−Pt(1)−N(1) | 89.1(2) | C(36)−Pt(1)−N(3) | 90.92(17) | C(35)−Pt(1)−N(2) | 89.41(12) |
| C(36)−Pt(1)−N(1) | 174.2(3) | C(42)−Pt(1)−N(3) | 177.0(2) | C(41)−Pt(1)−N(2) | 174.55(13) |
| N(2)−Pt(1)−N(1) | 85.5(2) | N(2)−Pt(1)−N(3) | 85.09(15) | N(3)−Pt(1)−N(2) | 85.19(10) |
| C(20)−C(1)−C(2) | 110.3(6) | C(20)−C(1)−C(14) | 113.1(4) | C(13)−Si−C(19) | 110.19(17) |
| C(20)−C(1)−C(14) | 112.2(5) | C(20)−C(1)−C(8) | 103.8(3) | C(13)−Si−C(1) | 106.93(16) |
| C(2)−C(1)−C(14) | 106.6(5) | C(14)−C(1)−C(8) | 111.1(4) | C(19)−Si−C(1) | 111.32(16) |
| C(20)−C(1)−C(8) | 110.5(5) | C(20)−C(1)−C(2) | 110.4(4) | C(13)−Si−C(7) | 109.48(16) |
| C(2)−C(1)−C(8) | 108.8(5) | C(14)−C(1)−C(2) | 105.2(3) | C(19)−Si−C(7) | 109.80(17) |
| C(14)−C(1)−C(8) | 108.2(5) | C(8)−C(1)−C(2) | 113.4(4) | C(1)−Si−C(7) | 109.06(17) |

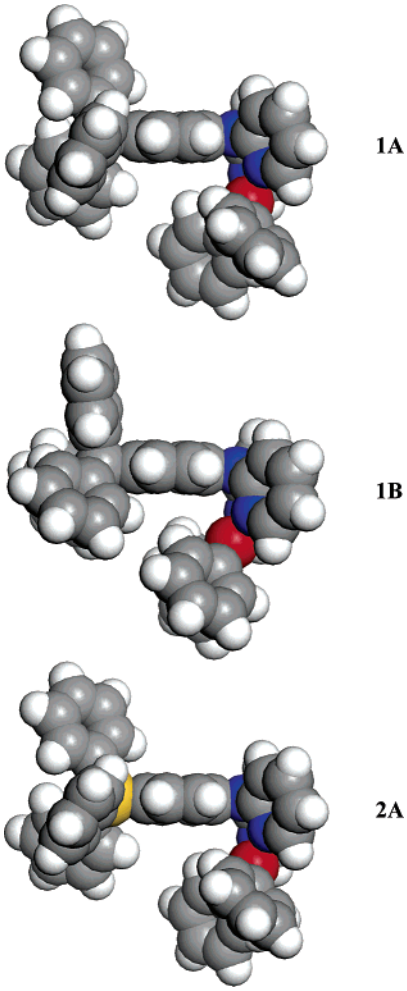


**Figure 2.** Space-filling diagrams showing the conformation difference of crystal **1A** (top), **1B** (middle), and **2A** (bottom). Pt: red; N: dark blue; Si: yellow.

**Table 3. Important Dihedral Angles for Crystals 1A, 1B, and 2A**

| crystal | dihedral angles between Py rings and the central Ph (deg) | dihedral angles between Ph rings and central Ph (deg) |
|---|---|---|
| **1A** | 83.7, 93.3 | 63.0, 72.1, 72.5 |
| **1B** | 82.0, 94.7 | 50.5, 61.6, 88.2 |
| **2A** | 82.9, 86.2 | 56.3, 57.1, 69.3 |

arrangement. For **1B**, a similar one-dimensional arrangement is observed. However, the Pt···H separation is much longer (3.50 Å), indicating a much weaker interaction than that in **1A**. Intermolecular Pt···Pt separation distance along the 1D chain is 14.13 Å for **1A** and 13.01 Å for **1B**. Perhaps, the most significant difference between the structures of **1A** and **1B** is the interactions between the 1D chains, in particular, the interactions between the phenyl group that has a weak H bond with the Pt center and the two pyridyl groups on the amino center. As shown by Figure 3, in **1A**, the phenyl group has an approximate "edge on" orientation with respect to the pyridyl rings from the neighboring chain with dihedral angles being 39.0° and 94.6°, respectively. The shortest atomic separation

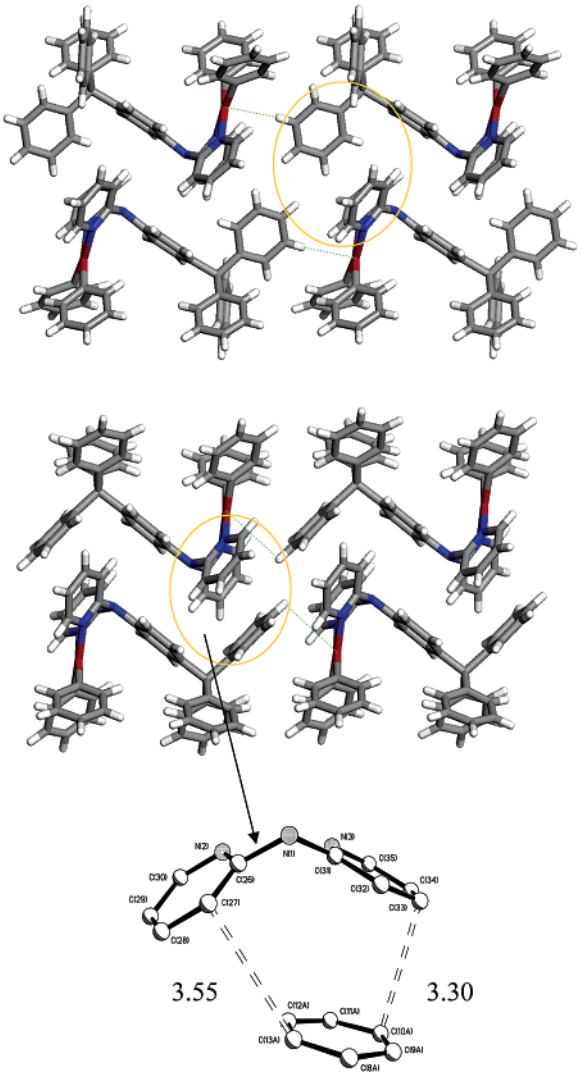


**Figure 3.** Diagrams showing Pt···H interactions (indicated by light blue lines) along the 1D chain and the interactions between the phenyl group and the pyridyl rings (indicated by the yellow circle) in the crystal lattice of **1A** (top) and **1B** (bottom). The diagram for **2A** is very similar to that of **1A** and can be found in the Supporting Information. Inset: diagram showing the relative orientation of the pyridyl rings and the phenyl ring in **1B** and the shortest atomic separation distances.

distance between the phenyl ring and two pyridyl rings in **1A** is 3.70 Å. In contrast, as shown in Figure 3, the phenyl group that is perpendicular to the central phenyl ring in **1B** is nearly parallel to one of the pyridyl rings (dihedral angle 19.2°), with the atomic separation distances ranging from 3.30 to 3.90 Å, an indication of strong $\pi$-stacking interactions. The same phenyl ring also has some interactions with the second pyridyl ring, as evidenced by the dihedral angle of 134.5° and several short atomic separation distances (3.55 and 3.59 Å). These $\pi$ interactions in **1B** are localized within two neighboring molecules, as shown in Figure 3, which could be described as a $\pi$-stacked "dimer". The difference in intermolecular interactions of **1A** and **1B** is clearly associated with their different molecular conformation. In terms of geometry, the conformation of the $CPh_3$ group in **1B** is evidently more constrained than that in **1A**, but this constraint is likely compensated by the formation of the $\pi$-stacked dimer. Another noteworthy feature observed in the extended structures of **1A** and **1B** is that the molecules are arranged in such a manner in the crystal lattice that the phenyl groups from neighboring molecules form a one-

(11) (a) Seward, C.; Wang, S. *Comments Inorg. Chem.* **2005**, *26*, 103, and references therein. (b) Jia, W.-L.; Wang, R.-Y.; Song, D. T.; Ball, S.; McLean, A.; Wang, S. *Chem., Eur. J.* **2005**, *11*, 832. (c) Seward, C.; Jia, W. L.; Wang, R. Y.; Enright, G. D.; Wang, S. *Angew. Chem., Int. Ed.* **2004**, *43*, 2933. (d) Pang, J.; Marcotte, E. J−P.; Seward, C.; Brown, R. S.; Wang, S. *Angew. Chem., Int. Ed.* **2001**, *40*, 4042.

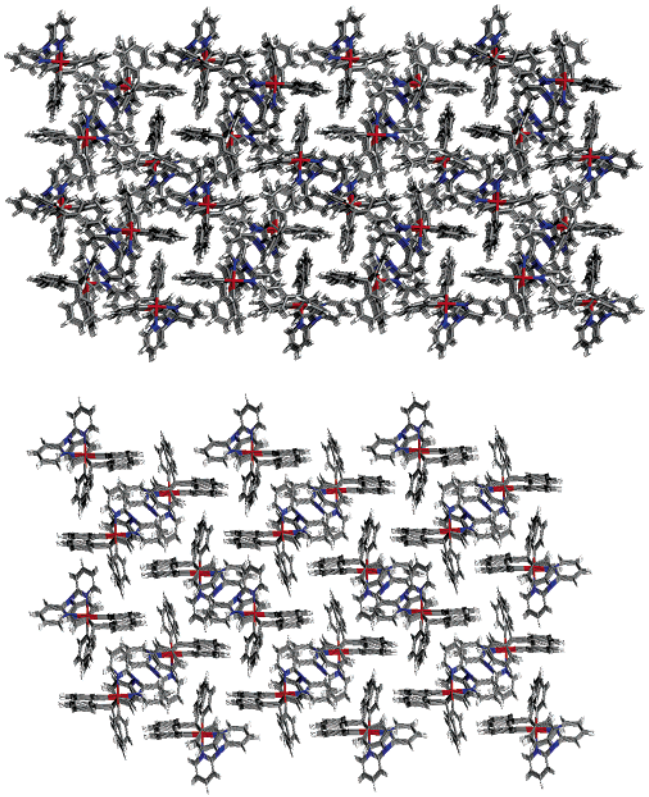

**Figure 4.** Crystal-packing diagrams showing the channels in the crystal lattices of **1A** and **1B** (projected down the *c* axis for **1A** and down the *a* axis for **1B**).

dimensional channel (Figures 4) with approximate dimensions of 3.0 Å × 3.0 Å for **1A** and 4.5 Å × 4.5 Å for **1B**. The volume of **1A** is about 2% less than that of **1B**, indicating that molecules in **1A** are more densely packed than those in **1B**. The density difference between the two polymorphs may account for their solubility difference.

The fact that both crystal forms were isolated under the same conditions indicates that they have a similar thermodynamic stability.[5] Because the main difference between the two polymorphs in terms of the molecular structure is the relative orientation of the phenyl groups, one might anticipate that sufficient thermal energy may be able to interconvert the two polymorphs. Attempts were therefore made to interconvert the crystals of **1A** and **1B** by heating the single crystals and monitoring the unit cell parameters' change by X-ray diffractions. However, up to 160 °C, no evidence of unit cell parameters' change was observed, which can be attributed to intermolecular interactions in the crystal lattice that stabilize both crystal forms.

Crystal **2A** is isostructral to **1A**. The *c* axis of the unit cell of **2A** is significantly longer than that of **1A**, due to the relatively longer Si−C bonds. The conformation of the $SiPh_3$ group in **2A** is identical to that of the $CPh_3$ group in **1A**. The 1D chain structure of **2A** is also similar to that of **1A**, with a Pt···H distance of 2.97 Å. The void square channel observed in **1A** is also present in **2A** with a slightly larger cross section of ~3.2 Å × 3.2 Å. The Pt−Si separation distance is 7.23 Å.

**Absorption Spectra.** The UV−vis spectra of compounds **1** and **2** recorded in $CH_2Cl_2$ are shown in Figure 5. There is no absorption beyond 400 nm for **1**. For **2** the absorption tails off at about 420 nm. The pattern of the absorption spectra resembles those of the corresponding free ligands,[9] an indication that the absorption bands are likely ligand-based transitions (localized

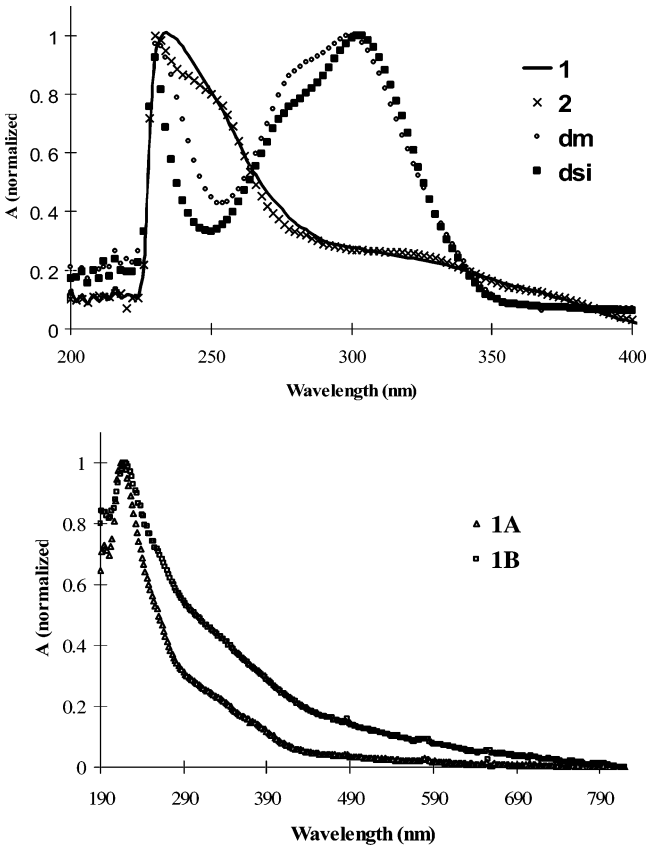


**Figure 5.** UV−vis absorption spectra of **1A** and **1B** in $CH_2Cl_2$ (top) and in the solid state (bottom).

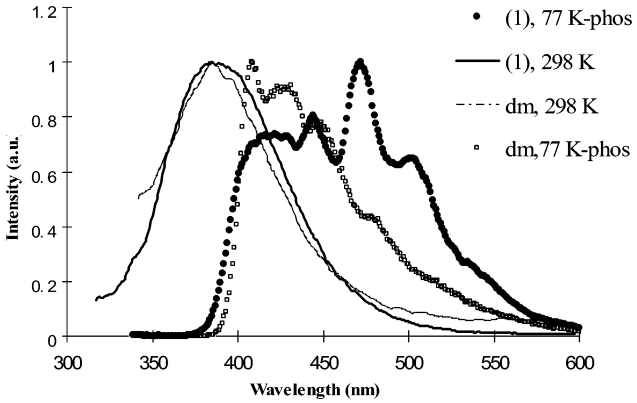


**Figure 6.** Emission spectra of **1** in $CH_2Cl_2$.

mostly on the 2,2′-dipyridylaminophenyl portion of the ligand, based on the results of molecular orbital calculations on the free ligands reported by us recently;[9] see Supporting Information). The major difference between the spectra of the free ligands and the corresponding Pt(II) complexes is the substantial decrease of the peak intensity at ~300 nm, relative to that at ~230 nm. To find out if the structural difference has any impact on the electronic properties of the polymorphs, the UV−vis spectra of **1A** and **1B** in the solid state were recorded and are shown in Figure 5. Although the spectra of **1A** and **1B** have similar features, the absorption of **1B** is clearly more intense in the region $\lambda > 300$ nm, which accounts for the yellow appearance of **1B** crystals. Because this long tail is absent in the solution spectrum of **1**, it must be the consequence of the molecular conformation or intermolecular interactions of **1B** in the crystal lattice. The UV−vis spectra of **2A** and **2B** are similar to those of **1A** and **1B**.

**Table 4. Absorption and Luminescent Data**

| compd | absorption (nm) ($\epsilon$, $M^{-1}$ $cm^{-1}$) | excitation (nm) | emission (nm) | decay lifetime ($\tau$, $\mu$s) | conditions |
|---|---|---|---|---|---|
| **1A** | 220 | 416 | 454 | | solid, 298 K |
| | | | 516 | 57(2) | solid, 298 K, time-resolved |
| | | 396 | 454 | | solid, 77 K |
| | | | 445 | 227.5(5) | solid, 77 K, time-resolved |
| | | | 467 | 111(1) | |
| | | | 496 | 61(3), 163(6) | |
| | 232 (24 000), 314 (sh, 6100), 335 (4400) | 301 | 391 | | $CH_2Cl_2$, 298 K |
| | | 329 | 411 | | $CH_2Cl_2$, 77 K |
| | | | 429 | | |
| | | | 470 | | |
| | | | 421 | 29(6) | $CH_2Cl_2$, 77 K, time-resolved |
| | | | 444 | 22(2) | |
| | | | 472, 503 | 331(3), 83(2) | |
| **2A** | 220 | 397 | 453 | | solid, 298 K |
| | | | 482 | 19 | solid, 298 K, time-resolved |
| | | | 505 | 18 | |
| | | 393 | 457 | | solid, 77 K |
| | | | 442 | 199 | solid, 77 K, time-resolved |
| | | | 470 | 214 | |
| | 230 (19 000), 315 (sh, 4800) | 311 | 385 | | $CH_2Cl_2$, 298 K |
| | | 339 | 430 | | $CH_2Cl_2$, 77 K |
| | | | 450 | | |
| | | | 450 | 53(5) | $CH_2Cl_2$, 77 K, time-resolved |
| | | | 475 | 234(10), 48(7) | |

**Luminescence in Solution.** Complex **1** (**1A** and **1B**) emits very weakly in fluid solution at 298 K with the emission maximum at 391 nm, which is identical to that of the free ligand and can be assigned as the ligand-based fluorescence. At 77 K, the emission spectrum of **1** has the maximum at 411 nm, again resembling that of the free ligand recorded under the same conditions. Using a time-resolved phosphorescent spectrometer, the phosphorescent spectrum of **1** in $CH_2Cl_2$ at 77 K was recorded. As shown in Figure 6, the phosphorescent emission bands of **1** are in the same blue-green region as the phosphorescent band of the free ligand dm,[9] except that the intensity of the low-energy emission bands is clearly enhanced in the complex. The decay lifetimes in solution at 77 K were determined to be in the regime of microseconds. Because of the similarity of the emission spectra of the free ligand dm and complex **1**, the observed phosphorescent emission of the complex is attributed to ligand-based transitions. The phosphorescent emission of the complex is however much more bright and more readily detectable than that of the free ligand, which can be attributed to the Pt atom, which enhances the phosphorescence of the ligand via the "heavy atom effect". The luminescent properties of **1** in solution are similar to those of closely related organoplatinum complexes based on star-shaped ligands of 2,2′-dipyridylamino aryl derivatives, which also display ligand-based blue-green phosphorescence at 77 K.[4g] The luminescent spectra of the silicon analogue **2** (**2A** and **2B**) in solution are similar to those of compound **1**. The relevant data are given in Table 4.

**Luminescence of the Polymorphs.** In the solid state, the two polymorph modifications of complexes **1A** and **1B** display distinct luminescent properties. When irradiated by UV light, **1A** emits a bright blue color, while **1B** is visually nonluminescent, as shown by the photograph of the two samples taken under UV light irradiation (Figure 8). At 298 K, the emission maximum of **1A** is at 454 nm, considerably red-shifted, compared to the solution spectrum. When dissolved and dispersed in a polymer matrix (PMMA), a similar emission spectrum with $\lambda_{max} = 450$ nm was observed at 298 K for both **1A** and **1B**. Using a time-resolved phosphorescent spectrometer, a broad phosphorescent band was recorded with $\lambda_{max} = 516$ nm and a decay lifetime of 57(2) $\mu$s. Therefore, the blue emission of **1A** at 298 K is best described as a mixture of fluorescence and phosphorescence with predominantly fluorescence character. The emission spectrum of **1A** at 77 K is almost identical to that at 298 K. However, using a time-resolved phosphorescent spectrometer, this broad emission band is resolved into three peaks, as shown in Figure 7, indicating that the emission of **1A** at 77 K is dominated by phosphorescence. The blue shift of the phosphorescent emission band at 77 K, compared to that at 298 K, is most likely caused by the increased environmental rigidity, which is consistent with the reduced thermal vibrational relaxation at low temperature.[12] Because the 77 K emission spectrum of **1A** is similar to the solution phosphorescent spectra of **1** and the free ligand dm at 77 K, we conclude that the emission of **1A** in the solid state is also based on ligand transitions.

Consistent with the behavior of **1A** and **1B**, the polymorph **2A** displays a blue emission when irradiated by UV light, while **2B** has no detectable emission. The luminescent data for **1A** and **2A** in solution and in the solid state are summarized in Table 4.

**Possible Causes for the Distinct Luminescent Properties of 1A and 1B.** To explain the different luminescent properties of **1A** and **1B**, the difference in molecular structures and the extended intermolecular interactions of **1A** and **1B** need to be considered. As shown by the crystal structures, the difference between the molecular structures of **1A** and **1B** is the conformation of one of the Ph rings on the $CPh_3$ group. The unusual perpendicular orientation by a phenyl group with respect to the central phenyl ring in **1B** (which causes considerable distortion of the C(8)−C(1)−C(20) bond angle (103.8(3)°) compared to that in **1A** (113.1(4)°) places it closer to the central phenyl ring than that in **1A**. To determine if the different orientation by the $CPh_3$ group has any possible impact on electronic properties of **1A** and **1B**, we performed ab initio molecular orbital calculations (Gaussian98) for both structures. Geometric parameters obtained

(12) (a) Wang, S.; Garzon, G.; King, C.; Wang, J. C.; Fackler, J. P., Jr. *Inorg. Chem.* **1989**, *28*, 4623. (b) Lees, A. J. *Chem. Rev.* **1987**, *87*, 711 (c) Ferraudi, G. J. *Elements of Inorganic Photochemistry*; John Wiley & Sons: New York, 1988.

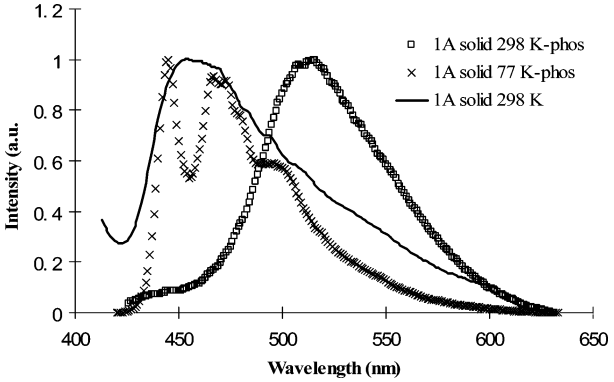


**Figure 7.** Emission spectra of **1A** in the solid state.

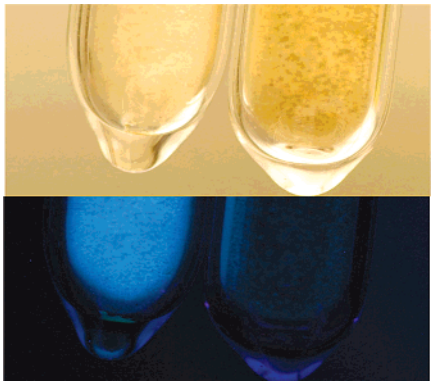

**Figure 8.** Photographs of **1A** (left) and **1B** (right) taken under ambient light (top) and UV light (bottom).

from X-ray diffraction analyses for both structures were used directly in the calculations. The calculations were performed with the B3LYP-G6-31* basis set employing a RHF (restricted Hartree−Fock) level of computation. To make the calculation feasible, the $PtPh_2$ portion was removed. (Attempts to calculate the entire structure using either the ab initio option or the DFT option were unsuccessful. The calculations did not converge. This is likely caused by the size of the molecule and the presence of the Pt atom.) The removal of the $PtPh_2$ portion is validated by the fact that it is similar in both structures and the luminescence appears to be ligand-centered transitions according to experimental data. The MO calculation results indicate that there is little difference in **1A** and **1B** in terms of the HOMO and LUMO energy.[13] However, as shown in Figure 9, although the LUMO level for both structures is essentially identical with contributions almost entirely from the $\pi^*$ orbitals of the two pyridyl groups, the HOMO level for the two structures is quite different: for **1A** it consists of the amino nitrogen $p_\pi$ orbital and the $\pi$ orbitals of the central phenyl ring, while for **1B** in addition to the amino nitrogen and the central phenyl ring $\pi$ orbitals, it has significant contributions from the $\pi$ orbitals of the perpendicular phenyl ring of the $CPh_3$ group. On the basis of the HOMO and LUMO appearance, the lowest ligand-

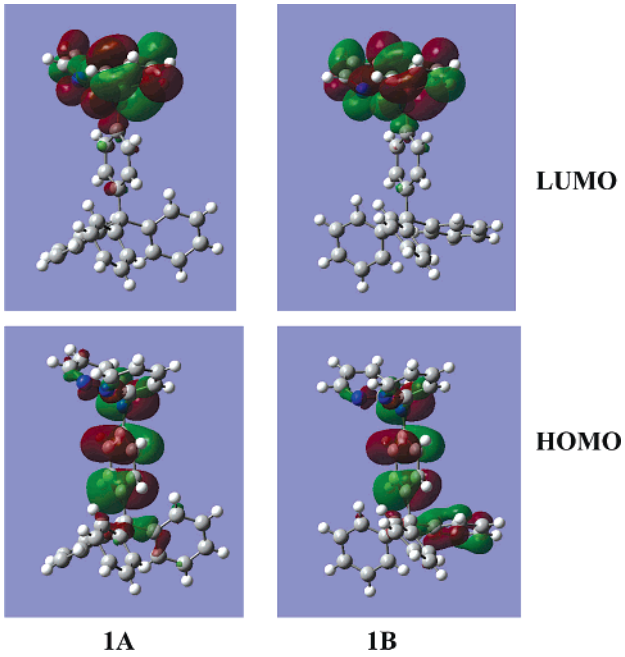


**Figure 9.** HOMO and LUMO diagrams for the dm ligand in **1A** and **1B**.

centered transition in **1A** and **1B** can be considered as internal charge transfer from the amino-phenyl portion to the pyridyls for **1A** and the amino-phenyl-CPh portion to the pyridyls in **1B**. As shown by the crystal structure of **1B**, the C−Ph group that is involved in the HOMO orbital is in close $\pi$-stacking contact (3.30−3.90 Å) with a pyridyl group from a neighboring molecule to form a "$\pi$-stacked dimer".[14] Because the LUMO orbital is made of the pyridyl atomic orbitals and the phenyl group has significant contributions to the HOMO level, such a close $\pi$ contact could lead to a facile intermolecular charge transfer between the C-Ph group and the pyridyl group and quench the emission,[15] which we believe is the most likely cause for the absence of emission by **1B**.

## Concluding Remarks

Previously known polymorphs involving organoplatinum[7,8] or organogold compounds[16] that display distinct electronic properties usually involve weak metal−metal interactions present in the crystal lattice. Examples of polymorphs such as **1A** and **1B** that are based on organoplatinum compounds and display distinct luminescent properties without the involvement of metal−metal interactions are still rare. Although the $PtPh_2$ group in **1A** and **1B** does not appear to be directly involved in the emission process, it clearly plays a role in the formation of the polymorphs **1A** and **1B** (and **2A** and **2B**) because in the absence of the $PtPh_2$ group, similar polymorphs were not observed for the free ligands dm and dsi. The molecular conformation difference observed in **1A** and **1B** is likely the

(13) The appearance of the HOMO and LUMO levels for the dm ligand in **1A** and **1B** is in sharp contrast with the MO calculation results obtained for the free ligand, where geometry optimization was performed and the pyridyl rings were found not to be perpendicular to the central phenyl ring, as they are in **1A** and **1B**. For the free ligand, the central phenyl ring and the 2,2′-dipyridylamino portion contribute almost equally to both HOMO and LUMO levels and no contributions from the $CPh_3$ group to either level were observed (see Supporting Information). The different MO calculation results for the free ligand and for the coordinated ligand are caused by the geometry change of the pyridyl rings (perpendicular to the central phenyl ring in **1A** and **1B**) and the conformational change of the $CPh_3$ ($SiPh_3$) group.

(14) (a) Amabillno, D. B.; Dietrich-Buchecker, C. O.; Livoreil, A.; Pérez-Garcia, L.; Sauvage, J. P.; Stoddart, J. F. *J. Am. Chem. Soc.* **1996**, *118*, 3905. (b) Yokoi, H.; Hatta, A.; Ishiguro, K.; Sawaki, Y. *J. Am. Chem. Soc.* **1998**, *120*, 12728. (c) Liao, P.; Itkis, M. E.; Oakley, R. T.; Tham, F. S.; Haddon, R. C. *J. Am. Chem. Soc.* **2004**, *126*, 14297. (d) Small, D.; Zaitsev, V.; Jung, Y.; Rosokha, S. V.; Head-Gordon, M.; Kochi, J. K. *J. Am. Chem. Soc.* **2004**, *126*, 13850.

(15) Lakowicz, J. R. *Principles of Fluorescence Spectroscopy*, 2nd ed.; Kluwer Academic/Plenum Publishers: New York, 1999.

(16) (a) Lu, W.; Zhu, N.; Che, C.-M. *J. Am. Chem. Soc.* **2003**, *125*, 16081. (b) White-Morris, R. L.; Olmstead, M. M.; Balch, A. L. *J. Am. Chem. Soc.* **2003**, *125*, 1033.

consequence of intermolecular interactions in the two crystal lattices, which, albeit subtle, clearly have a dramatic impact on the luminescent properties of the materials in the solid state.

**Acknowledgment.** We thank the Natural Sciences and Engineering Research Council of Canada for financial support.

**Supporting Information Available:** Diagrams showing the molecular structures of **1B** and **2A** with labeling schemes, a diagram showing the intermolecular interactions of **2A**, diagrams showing the $\pi$-stacked dimer in the crystal lattices of **1B**, the emission spectra of **2A**, the HOMO and LUMO diagrams for the free ligands obtained with geometry optimization, and a complete listing of crystal data for **1A**, **1B**, and **2A**, including tables of atomic coordinates, thermal parameters, bond lengths and angles, and hydrogen parameters. This material is available free of charge via the Internet at http://pubs.acs.org.

OM0600184